

# Multi-Set Point Intermittent Contact (MUSIC) Mode Atomic Force Microscopy of Oligothiophene Fibrils

Eike-Christian Spitzner,<sup>\*,†</sup> Christian Riesch,<sup>†</sup> Ruth Szilluweit,<sup>‡</sup> Liangfei Tian,<sup>‡,§</sup> Holger Frauenrath,<sup>‡</sup> and Robert Magerle<sup>\*,†</sup>

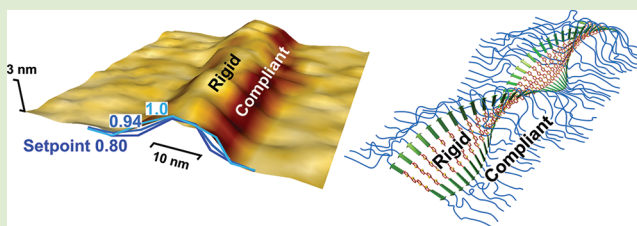
<sup>†</sup>Chemische Physik, Technische Universität Chemnitz, D-09107 Chemnitz, Germany

<sup>‡</sup>Institute of Materials, École Polytechnique Fédérale de Lausanne (EPFL), 1015 Lausanne, Switzerland

<sup>§</sup>Department of Materials, ETH Zürich, 8093 Zürich, Switzerland

## Supporting Information

**ABSTRACT:** We developed MUSIC-mode atomic force microscopy (AFM) to emulate intermittent contact mode AFM without a feedback loop and in the absence of lateral forces. This single-pass approach is based on maps of amplitude-phase-distance curves and allows the height and phase images to be simultaneously obtained for almost any amplitude set point. This is advantageous for determining the shape and nanomechanical properties of very soft and fragile samples. As an example, we studied supramolecular aggregates of oligothiophenes, which form  $\approx 15$  nm wide fibrils with a rigid core and a soft shell.



Intermittent contact (IC) mode atomic force microscopy (AFM),<sup>1,2</sup> also known as amplitude modulation or tapping mode AFM, is widely used for imaging individual nano-objects.<sup>3,4</sup> The imaging of very soft and fragile samples with IC-mode AFM, however, remains a challenge because the detailed results strongly depend on the chosen amplitude set point  $A/A_0$ , where  $A_0$  is the amplitude of the freely oscillating system and  $A$  is the damped amplitude.<sup>5,6</sup> Whereas a high amplitude set point is desirable for an unperturbed IC-mode AFM height image, a lower set point results in a better contrast in the IC-mode AFM phase image.<sup>5</sup> The topographic information is often affected by the indentation of the tip into the specimen,<sup>7</sup> and artifacts in both the phase image and the height image are caused by the finite response time of the amplitude feedback loop.<sup>8,9</sup> Different techniques have been developed to resolve the aforementioned problems, but they typically require multiple and time-consuming measurements at different amplitude set points<sup>5–7</sup> or a modified AFM setup<sup>8,9</sup> to address all of the problems.

Here, we present the use of multi-set point intermittent contact (MUSIC) mode AFM as a single-pass approach for simultaneously obtaining the height and phase image information for almost any amplitude set point ratio  $A/A_0$ . For this purpose, we use maps of amplitude-phase-distance (APD) curves to emulate IC-mode AFM without a feedback loop and in the absence of lateral forces. The sample is mapped by pointwise measuring both the amplitude and the phase while reducing the tip-sample distance until a specified minimum amplitude  $A_{\min}$  is reached. In this way, we can obtain the true sample surface,<sup>7</sup> the tip indentation,<sup>10</sup> quantitative information about the tip-sample interaction,<sup>11–14</sup> and depth-resolved IC-mode AFM images.<sup>15</sup>

To demonstrate the advantages of MUSIC-mode, we investigated self-assembled nanofibrils formed from oligothiophene derivatives (Figure 1a) that may be of interest as organic

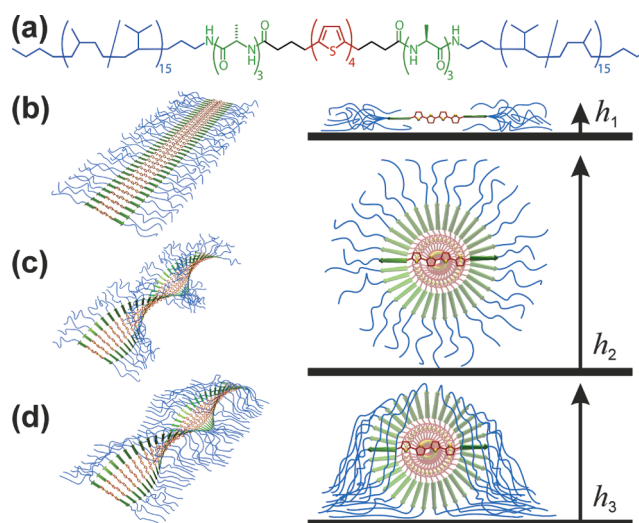


**Figure 1.** (a) Molecular structure of the studied oligothiophene derivative. (b–d) Sketches of structural models for the arrangement of the molecules within a fibril deposited on a substrate (left, oblique view; right, cross section).

Received: January 12, 2012

Accepted: February 15, 2012

Published: February 23, 2012

semiconducting nanowires.<sup>16</sup> The molecules comprise a quarterthiophene core with terminally attached oligopeptides and flexible, hydrophobic polymer segments (hydrogenated polyisoprene). In organic solvents, they self-assemble into one-dimensional aggregates (fibrils) promoted by hydrogen bonding. MUSIC-mode AFM allowed us to determine the shape and nanomechanical properties of these nanofibrils with nanometer resolution in a time-efficient manner. Our results show that the nanofibrils have a rigid core that is formed from stacked oligothiophene segments (Figure 1a, red) and their oligopeptide substituents (Figure 1a, green). This helically twisted core is embedded into a soft shell of the terminally attached flexible polymer segments (Figure 1a, blue), which also wet the substrate (Figure 1d). In the following, we present the results for MUSIC-mode AFM imaging and compare them to images obtained by IC-mode AFM. Figure 2a shows a

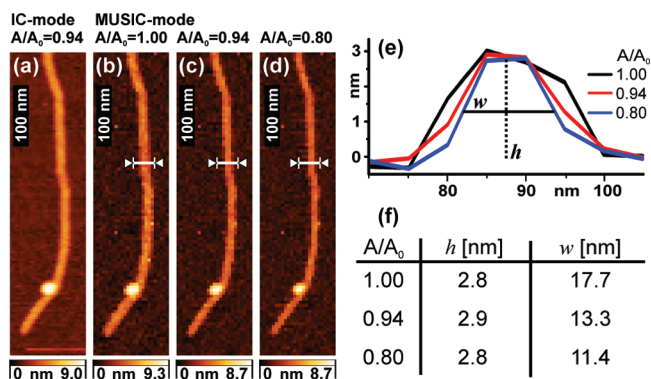


**Figure 2.** (a) Conventional IC-mode AFM height image of an oligothiophene fibril (set point  $A/A_0 = 0.94$ ) deposited on a silicon-oxide-covered silicon substrate and (b–d) MUSIC-mode AFM height images at the set points  $A/A_0 = 1.00$ ,  $0.94$ , and  $0.80$ , respectively. (e) Cross sections along the white lines shown in (b–d). (f) Height  $h$  relative to the substrate and width  $w$  of the fibril at half height.

conventional IC-mode AFM height image of an oligothiophene fibril. The wire-like shape of the aggregate, with almost constant height, is clearly visible with the exception of an irregularity in the lower part of the fibril. The height image was taken at the highest set point that allowed for stable imaging in conventional IC-mode ( $A/A_0 = 0.94$ ). Figure 2b–d show the MUSIC-mode AFM height images for different set points  $A/A_0$ . The height image for  $A/A_0 = 1.00$  corresponds to the shape of the unperturbed sample surface, determined as in ref 7. Cross sections that were determined as averages of four adjacent rows of pixels next to the white markers in Figure 2b–d are shown in Figure 2e. We consider the full width at half-maximum to be an approximation of the fibril's width, but one has to keep in mind that the measured profile is a convolution of the actual height profile and the shape of the tip. In our case, the full width at half-maximum decreases from 17.7 to 11.4 nm with decreasing set point values, whereas the height of the fibril remains constant. This indicates the presence of softer material located along both edges of the fibril, which allows the tip to indent deeper at these points than on top of the fibril. Figure 3 shows a conventional IC-mode AFM phase image for  $A/A_0 = 0.94$  (Figure 3a) and MUSIC-mode phase images for the same set point (Figure 3b) as well as for  $A/A_0 = 0.80$  (Figure 3c). Higher phase values correspond to a more rigid material. The conventional IC-mode AFM phase image appears as if illuminated from the left-hand side with higher phase values

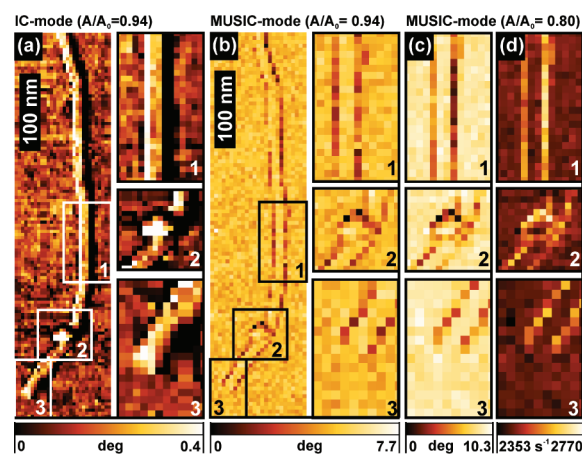


**Figure 3.** (a) Conventional IC-mode AFM phase image ( $A/A_0 = 0.94$ ) and (b) MUSIC-mode AFM phase image of the same fibril, as shown in Figure 2 for the same set point. (c) MUSIC-mode phase and (d) the effective damping parameter  $\alpha_{\text{eff}}/m$  of the details (1–3) for a set point of  $A/A_0 = 0.80$ . Detail (1) shows a straight part of the fibril, detail (2) a defect structure, and detail (3) the fibril's terminus.

at the left edge and lower values at the right edge of the fibril. This is a well-known imaging artifact caused by the finite response time of the tip-height feedback loop.<sup>17</sup> Scanning across large gradients in the sample topography with conventional IC-mode AFM often results in discontinuities in  $A/A_0$ , leading to the wrong impression of asymmetric material properties in the IC-mode phase image. The strength of this effect depends on the tip scanning direction and velocity as well as the feedback loop parameters. Due to the pointwise measurement of APD curves without a feedback loop, the MUSIC-mode AFM phase images are not affected by this type of artifact. The phase images emulated for the set points  $A/A_0 = 0.94$  and  $A/A_0 = 0.80$  (Figure 3b,c) have a higher contrast with less noise than the conventional IC-mode phase image. Both clearly reveal a symmetric distribution of mechanical properties perpendicular to the fibril axis, with a rigid core symmetrically lined with softer material along both edges, as indicated by the lower phase values. The fibril's terminus is not covered with any soft material [Figure 3c, detail (3)]. Another fibril that was oriented perpendicular to the one shown in Figure 3 was measured with the same tip and exhibited the same structure at its terminus (see Supporting Information). This excludes the possibility that the discussed findings are artifacts resulting from the tip shape. The MUSIC-mode AFM phase image for  $A/A_0 = 0.8$  (Figure 3c) shows a higher contrast and less noise than that for  $A/A_0 = 0.94$ , which agrees with the often observed set point dependence of IC-mode AFM phase images.<sup>5–7,18</sup> Our interpretation of the phase contrast confirms the conclusions drawn from the MUSIC-mode AFM height images at different set points that were obtained in the same measurement run. It is also consistent with a quantitative analysis of tip–sample interaction according to ref 12. Lower phase values correspond to a higher effective damping parameter  $\alpha_{\text{eff}}/m$  (Figure 3d).

The detailed nanomechanical information obtained from a single MUSIC-mode AFM measurement indicates which one of the several possible nanofibril models is most likely correct. Previous investigations of related compounds<sup>19,20</sup> as well as spectroscopic results suggest a helical stacking of the oligothiophene chromophores. Some plausible structural models for fibrils deposited on a solid substrate include flat

tapes (Figure 1b), stacks of tapes, as well as helical fibrils with either a swollen polymer shell (Figure 1c) or polymer segments in the collapsed state (Figure 1d). From the MUSIC-mode AFM results, the model of single flat tapes can be excluded because the measured height of  $h = 2.8$  nm does not agree with the expected height  $h_1 = 1.5$  nm. Stacks of flat tapes cannot be categorically ruled out, but are not supported by investigations of related compounds.<sup>19</sup> Furthermore, because the morphology of all observed fibrils is uniform, the presence of two-tape stacks would raise the question of what limits further vertical aggregation. The model of a helical fibril with a swollen polymer shell (Figure 1c) can be unambiguously ruled out because the expected height of  $h_2 = 15$  nm disagrees with the measured height and because no soft material is observed on top of the rigid core. The measured fibril height of 2.8 nm is in good agreement with the length of the more rigid central part of the molecules (oligopeptide-oligothiophene-oligopeptide), which has a contour length of 4 nm ( $h_3$ ). At the terminus of the fibril, the helically twisted tape may be adsorbed flat on the substrate, which does not give the polymers the freedom to explore the space around the terminus. The helical pitch is apparently not resolved in the AFM images. To conclude, the model of a collapsed helix (Figure 1d) describes the MUSIC-mode AFM results best.

In summary, MUSIC-mode AFM uses the pointwise measurements of amplitude and phase as a function of the tip-sample distance to emulate IC-mode AFM for multiple set points in only one single-pass measurement run. This procedure resolves the dilemma of conventional IC-mode AFM in which high amplitude set points are required for minimizing the tip-indentation artifacts in height images, but low set points are required for maximizing the contrast in phase images.<sup>5–7</sup> MUSIC-mode AFM does not entail lateral forces and it is not affected by artifacts caused by the tip-height feedback loop, as in conventional IC-mode AFM. Another advantage is that all the obtained height and phase images show exactly the same location and no image registration is needed. Furthermore, the APD data allow for a quantitative analysis of the tip-sample interaction.<sup>11,12,15</sup> This complements other AFM-based methods for mapping nanomechanical properties.<sup>21,22</sup> Because the instrument was in no way optimized for this kind of measurement, we see much room for improvement, especially by using an AFM setup designed for high-speed imaging. Compared to sequentially imaging a sample at different set points, MUSIC-mode AFM is very time efficient. The data shown here were measured in 30 min. Because the data acquisition protocol is already implemented in most commercial atomic force microscopes, we consider MUSIC-mode AFM to be a versatile method for studying supramolecular and polymeric nanostructures as well as biological matter.

## MATERIALS AND METHODS

The oligothiophene derivatives were synthesized following the principles described in ref 23. In solution, the molecules self-assemble into fibrillar aggregates. The fibrils were deposited by spin-casting from a 1,1,2,2-tetrachloroethane solution onto a polished silicon-oxide-covered silicon substrate. All AFM measurements were performed under ambient conditions using a silicon cantilever (Pointprobe NCH, NanoWorld AG, Neuchâtel, Switzerland) with resonance frequency  $\omega_0 = 295.779$  kHz, spring constant  $k = 32.3$  N/m (determined as in ref 24), and quality factor  $Q = 640$ . The AFM used was a NanoWizard I (JPK Instruments AG, Berlin, Germany). An array of 25 by 100 APD curves was measured on an area of 125 nm by 500 nm. The free

amplitude far away from the surface ( $\approx 5 \mu\text{m}$ ) was 24 nm,  $A_0 = 19$  nm,  $A_{\text{min}} = 15$  nm, and the drive frequency  $\omega = 0.9995\omega_0 = 295.631$  kHz. This set of data incorporates the height and phase values as a function of the damped amplitude  $A$  down to  $A_{\text{min}}$ . Therefore, the MUSIC-mode AFM height images for a large range of set points (here 1.00 to 0.79) can be reconstructed. The precise determination of  $A_0$  and therefore of  $A/A_0$  is not trivial in conventional IC-mode AFM (see Supporting Information for a more detailed discussion). In MUSIC-mode AFM, the free amplitude  $A_0$  is determined for every single pixel right before the onset of the tip-sample interaction. This leads to a much more accurate set point determination, which is only limited by the precision of the amplitude detection. In this way, it is also possible to correct for changes of the free amplitude during imaging. The height image for  $A/A_0 = 1.00$  corresponds to the shape of the unperturbed sample surface, determined as in ref 7. It is the position where attractive forces first cause a phase change when the tip approaches the surface. The value  $A/A_0 = 1.00$  also occurs at a smaller tip-sample distance, where attractive and repulsive interactions cancel each other. However, at this point, the tip indents into the sample and therefore does not represent the unperturbed surface.

## ASSOCIATED CONTENT

### Supporting Information

We present a detailed discussion concerning the determination of the amplitude set point in AM-AFM. We also show a MUSIC-mode height and a phase image of another oligothiophene fibril in the vicinity of the fibril shown in Figures 2 and 3. This material is available free of charge via the Internet at <http://pubs.acs.org>.

## AUTHOR INFORMATION

### Corresponding Author

\*E-mail: eike-christian.spitzner@physik.tu-chemnitz.de; robert.magerle@physik.tu-chemnitz.de.

### Notes

The authors declare no competing financial interest.

## ACKNOWLEDGMENTS

The acquisition of the atomic force microscope was funded by the Volkswagen Foundation and the Deutsche Forschungsgemeinschaft. HF, LT, and RS acknowledge funding from the European Research Council (ERC Grant 239831, OrgElNano-CarbMater), the Swiss National Science Foundation (SNF Grant 200020-121812), and the ETH Research Grant TH 20 07-1.

## REFERENCES

- (1) Zhong, Q.; Inniss, D.; Kjoller, K.; Elings, V. B. *Surf. Sci. Lett.* **1993**, *290*, L688–L692.
- (2) García, R.; Pérez, R. *Surf. Sci. Rep.* **2002**, *47*, 197–301.
- (3) Magonov, S. N.; Whangbo, M.-H. *Surface Analysis with STM and AFM*; Wiley-VCH: Weinheim, 1996.
- (4) Tsukruk, V. V., Ed. *Macromolecular symposia. Advances in Scanning Probe Microscopy of Polymers*; Wiley-VCH: Weinheim, 2001; Vol. 167.
- (5) Bar, G.; Thomann, Y.; Brandsch, R.; Cantow, H.-J.; Whangbo, M.-H. *Langmuir* **1997**, *13*, 3807–3812.
- (6) O'Dea, J. R.; Buratto, S. K. *J. Phys. Chem. B* **2011**, *115*, 1014–1020.
- (7) Knoll, A.; Magerle, R.; Krausch, G. *Macromolecules* **2001**, *34*, 4159–4165.
- (8) Jeong, Y.; Jayanth, G. R.; Jhiang, S. M.; Menq, C.-H. *Appl. Phys. Lett.* **2006**, *88*, 204102.
- (9) Rogers, B.; Manning, L.; Sulchek, T.; Adams, J. D. *Ultra-microscopy* **2004**, *100*, 267–276.

- (10) Höper, R.; Gesang, T.; Possart, W.; Hennemann, O.-D.; Boseck, S. *Ultramicroscopy* **1995**, *60*, 17–24.
- (11) García, R.; Gómez, C. J.; Martínez, N. F.; Patil, S.; Dietz, C.; Magerle, R. *Phys. Rev. Lett.* **2006**, *97*, 016103.
- (12) Schröter, K.; Petzold, A.; Henze, T.; Thurn-Albrecht, T. *Macromolecules* **2009**, *42*, 1114–1124.
- (13) de Beer, S.; van den Ende, D.; Mugele, F. *Nanotechnology* **2010**, *21*, 325703.
- (14) Ye, Z.; Zhao, X. *J. Microsc.* **2010**, *238*, 27–35.
- (15) Spitzner, E.-C.; Riesch, C.; Magerle, R. *ACS Nano* **2011**, *5*, 315–320.
- (16) Hoeben, F. J. M.; Jonkheijm, P.; Meijer, E. W.; Schenning, A. P. *H. J. Chem. Rev.* **2005**, *105*, 1491–1546.
- (17) Sulchek, T.; Hsieh, R.; Adams, J. D.; Yaralioglu, G. G.; Minne, S. C.; Quate, C. F.; Cleveland, J. P.; Atalar, A.; Adderton, D. M. *Appl. Phys. Lett.* **2000**, *76*, 1473–1475.
- (18) Kumar, B.; Pifer, P. M.; Giovengo, A.; Legleiter, J. *J. Appl. Phys.* **2010**, *107*, 044508–044508–8.
- (19) Frauenrath, H.; Jahnke, E. *Chem. Eur. J.* **2008**, *14*, 2942–2955.
- (20) Jahnke, E.; Severin, N.; Kreutzkamp, P.; Rabe, J. P.; Frauenrath, H. *Adv. Mater.* **2008**, *20*, 409.
- (21) Sahin, O.; Magonov, S.; Su, C.; Quate, C.; Solgaard, O. *Nat. Nanotechnol.* **2007**, *2*, 507.
- (22) Adamcik, J.; Berquand, A.; Mezzenga, R. *Appl. Phys. Lett.* **2011**, *98*, 193701.
- (23) Tian, L.; Szilluweit, R.; Marty, R.; Bertschi, L.; Zerson, M.; Spitzner, E.-C.; Magerle, R.; Frauenrath, H. **2012**, *RSC Chemical Science*, DOI: 10.1039/C2SC00977C.
- (24) Sader, J. E.; Chon, J. W. M.; Mulvaney, P. *Rev. Sci. Instrum.* **1999**, *70*, 3967–3969.